Impact of deep foundations on high-rise buildings during seismic events

C. Alanoca, R. Mangushev & L. Kondratieva
Saint Petersburg State University of Architecture and Civil Engineering (SPbGASU), Saint petersburg, Russia

ABSTRACT: The seismic behaviour of high-rise buildings on soft soils is influenced by dynamic soil-structure interaction (DSSI). However, common numerical models often neglect seismic ground pressure on underground structures due to kinematic and inertial effects. This study evaluates DSSI impacts, showing that piled raft foundations increase shear forces at the base of high-rise buildings. Using PLAXIS 3D, results were compared with Eurocode 8 analytical calculations, This study highlights the necessity of integrating new soil-foundation-structure interaction models and seismic ground response analysis into engineering practice to enhance the safety and efficiency of high-rise buildings constructed on soft soils, particularly under seismic acceleration of 0.025g at the surface (low-intensity earthquake), focusing on key seismic factors such as frequency, amplitude and acceleration.

1 INTRODUCTION

This study investigated the seismic response of high-rise buildings with deep foundations in soft soils, focusing on dynamic soil-structure interaction. Two foundation types—shallow foundations with jet grouting and piled rafts—were compared using PLAXIS 3D and FEM, validated against Eurocode 8. Results highlighted the role of pile foundations in load transfer and the impact of soil improvement on seismic performance. The findings contributed to optimizing foundation design and enhancing seismic safety, particularly under low-intensity earthquakes (0.027g PGA at the surface of the ground).

2 SETTING THE TASK

2.1 *Modelling Stages*

The study was carried out in two stages.

Stage 1: A representative soil profile was modelled using the Hardening Soil Small-Strain (HS-small) model in PLAXIS 3D to capture nonlinear soil behaviour with stress-dependent stiffness and plasticity. The shear wave velocity was calculated to classify the soil per Eurocode 8.

Stage 2: A high-rise building was subjected to seismic motion to assess the impact of two foundation types: shallow foundation reinforced with jet grouting and piled raft. Shear forces at the foundation interface were analysed using PLAXIS 3D and manually verified per Eurocode 8. The Eurocode 8 elastic response spectrum (EN 1998-1:2004) was used for structural compliance evaluation.

2.2 *Assumptions and Limitations*

The analysis was based on specific assumptions and constraints. It focused on a single seismic event and two soil types, limiting the scope of a comprehensive spectral analysis. Soil properties were assumed to represent a specific mass state, and a simplified two-layer model was used, which may not fully capture real conditions. Kinematic pile-soil-structure interaction and pile bending moments were not analysed, despite Eurocode 8, Part 5, requiring design for both inertial and kinematic forces.

Liquefaction and groundwater gradients were also excluded. Rayleigh damping was applied to model soil damping, omitting geometric damping in the PLAXIS model. Structural elements were assumed to behave elastically. These constraints define the study's scope and suggest areas for future research.

2.3 *The HS-Small Model in Seismic Analysis*

The HS-small model is a modification of the HS model that accounts for increased soil stiffness at low strain levels. Soil stiffness is significantly higher at very low strains, causing a nonlinear strain-stiffness relationship. To address this, the HS-small model introduces two additional parameters:

Reference small-strain shear modulus, G_0^{ref}, which represents the initial stiffness of the soil at very small strains (typically in the range of $1x10^{-6}$).

Shear strain level, $\gamma_{0.7}$, at which the small-strain shear modulus reduces to approximately 70% of its initial value.

The small-strain shear modulus is defined as:

$$G_0 = G_0^{ref} \left(\frac{c.\cos\varphi - \sigma_3' \sin\varphi}{c.\cos\varphi + P_{ref} \sin\varphi} \right)^m \quad (1)$$

where G_0^{ref}= reference small-strain shear modulus; σ_3'= effective confining stress; c = cohesion; φ = friction angle; P_{ref} = reference pressure, m = stress exponent.

The stress-strain behaviour for small strains follows the hyperbolic model proposed by Hardin and Drnevich (1972):

$$\frac{G_s}{G_0} = \frac{1}{1+\left|\frac{\gamma}{\gamma_{0.7}}\right|} \quad (2)$$

where G_s= secant shear modulus at a given strain level; G_0= initial small-strain shear modulus (when strain is near zero); γ = shear strain; $\gamma_{0.7}$ = shear strain level at which the modulus reduces to 70% of its initial value.

2.4 *Typical pile foundation damage during earthquake*

Pile foundations enhance bearing capacity and minimize differential settlement in soft soils. During earthquakes, lateral seismic loads alter forces on piles due to ground deformation. Most failures stem from soil liquefaction, making studies on damage in non-liquefiable soils rare (Martin & Lam 1995).

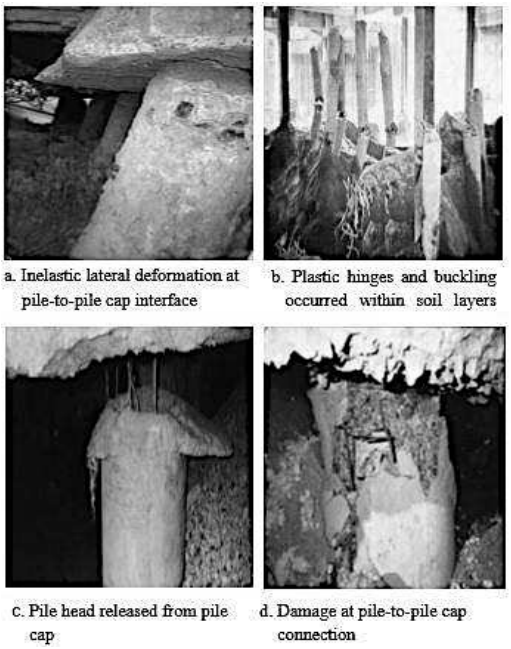

Figure 1. Pile foundation damage due to strong earthquakes (Hamada 1991; Mizuno 1987). Figures from (Teguh, 2006)

However, several authors have studied how to estimate the sectional forces on piles during earthquakes in different situations. Various programs are used for this purpose, and some countries have conducted more research on earthquakes due to the significant structural problems caused by dynamic loads.

Hamada in 2015 conducted shake table and lateral load tests on piles in a centrifuge to assess the impact of ground deformation on bending moments.

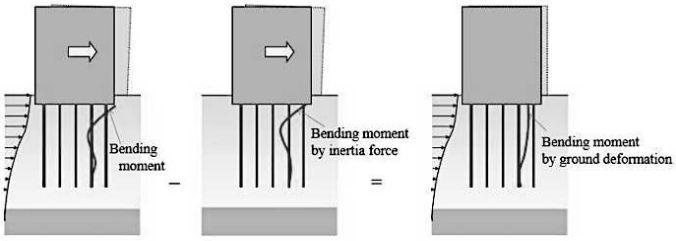

Figure 2. Estimation of bending moment in piles caused by ground deformation (J. Hamada, 2015)

The study proposed estimating dynamic bending moments by subtracting static bending moments from those measured in shaking table tests. This approach allows for estimating shear forces under dynamic conditions in a similar manner.

3 CONSTRUCTIONS OF FEM MODELS AND PARAMETERS

A total of two models were used for the analysis.

Model 1: Tall building structure with shallow foundation and jet grouting;

Model 2: Tall building structure with piled raft.

3.1 *Concept and geometry*

The soil profile was modelled as a cube with dimensions 270 m × 270 m × 220 m, extending 220 m down to the bedrock. The upper 30 m layer consisted of soft sand, while the next 190 m layer was made of relatively stiff sand. The structure was a tall building with a base area of 5929 m² and a height of 480 m, with an underground structure of 5929 m² and a depth of 10 m (2 floors, each 5 m deep). The shallow foundation had dimensions of 77 m × 77 m × 4 m. Piles extended from the shallow foundation into the coarse sand layer, with a length of 80 m.

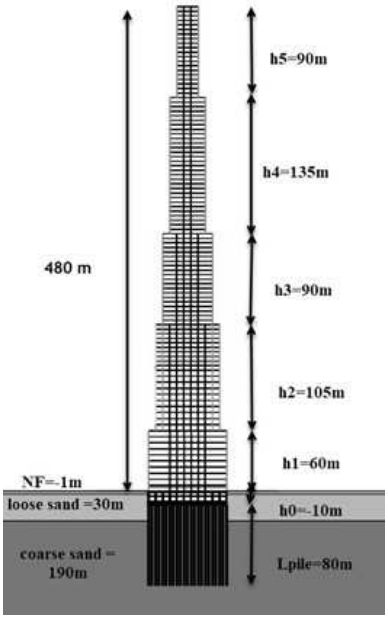

Figure 3. Schematic representation of the model concept with structure in AutoCAD

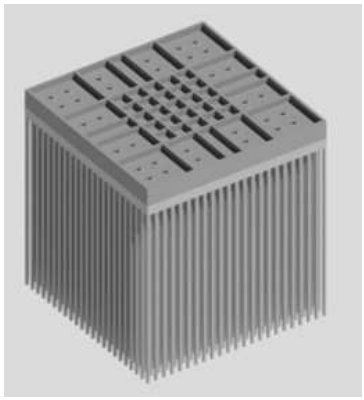

Figure 4. Structure foundation with piled-raft in REVIT

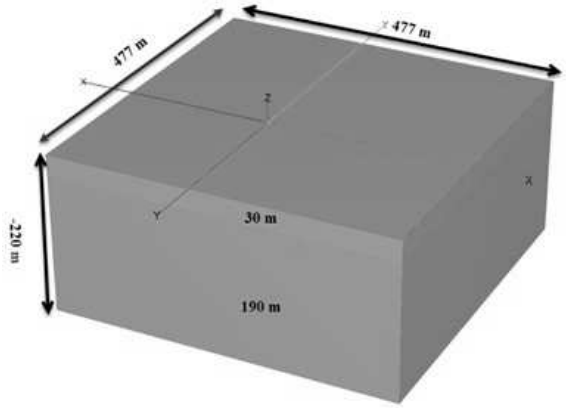

Figure 5. Soil profile without structure in PLAXIS

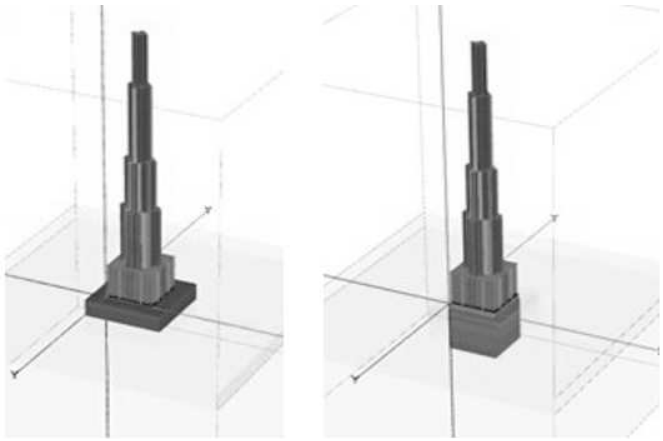

Figure 6. Tall building structure with shallow foundation and jet grouting, piled raft in PLAXIS 3D

3.2 *Material properties*

The key material properties of soil layers, structural elements, and foundation components were detailed in the followings tables to ensure accurate numerical simulations and design validation.

These parameters served as the foundation for evaluating structural performance and soil-structure interaction, ensuring a reliable and resilient design.

Table 1. Soil parameters for HS-small model.

Parameter	Name	Upper loose sand layer	Lower coarse sand layer	Unit
General				
Material Model	Model	HS small	HS small	-
Type of material behaviour	Type	Undrained (A)	Undrained (A)	-
Soil unit weight above phreatic level	γ_{unsat}	16	20	kN/m^3
Soil unit weight below phreatic level	γ_{sat}	16	20	kN/m^3
Parameters				
Secant stiffness in standard drained triaxial test	E_{50}^{ref}	10.5	60.0	MPa
Tangent stiffness for primary oedometer loading	E_{oed}^{ref}	7.0	40.0	MPa
Unloading/ reloading stiffness	E_{ur}^{ref}	35.0	200.0	MPa
Power for stress-level dependency of stiffness	m	0,5	0,5	-
Cohesion	c'_{ref}	0	0	KPa
Friction angle	φ'	32	38	°
Dilatancy angle	ψ	2	8	°
Shear strain at which G_s=0,722G_o	$\gamma_{0.7}$	0,1078*10^{-3}	0,2190*10^{-3}	-
Shear modulus at very small strains	G_0^{ref}	75,54*10^3	123,2*10^3	KPa
Poisson´s ratio	υ'_{ur}	0,2	0,2	-
Reference pre-consolidation pressure	Pref	100	100	KPa
K0- for normally consolidated soil	K0	0.4701	0.3843	

Table 2. Material Properties of basement, slab and wall of the structures (set type: Plate)

Parameter	Symbol	Unit	Basement, floors, slab and walls of both structures
Material Type			Elastic Isotropic
Structure of concrete unit weight	γ	kN/ m^3	25
Modul elasticity	E_1	kN/ m^2	30×10^6
Modul elasticity	E_2	kN/ m^2	30×10^6
Coefficient's Poisson	v_{12}	-	0.2
Modul of Rigidity in Shear	G_{12}	kN/ m^2	12.5×10^6
Modul of Rigidity in Shear	G_{13}	kN/ m^2	12.5×10^6
Modul of Rigidity in Shear	G_{23}	kN/ m^2	12.5×10^6
Raleigh Damping	α	-	0.2320
Raleigh Damping	β	-	8.000E-3

Table 3. Building loads on the different floors in kN/m^2

Parts of the structures	Weights	Unit
Basement	4	*kN/m^2*
Slab Underground (1-2 floors)	4	*kN/m^2*
Slab and floors in the tower (1-100 floors)	3	*kN/m^2*

Table 4. Material Properties of columns (set type: Beams)

Parameters	Symbol	Column	Unit
Material Type	Type	Elastic	-
Spacing	Lspacing	m	*7*
Structure of concrete unit weight	γ	kN/ m^3	25
Modul elasticity	E	kN/ m^2	30×10^6
Raleigh Damping	α		0.2320
Raleigh Damping	β		8.000E-3

Table 5. Input parameters of embedded beam

Parameter	Symbol	Unit	Pile
Material model			Elastic
Young's modulus	E	kN/m^2	30.00E6
Unit weight	γ	kN/m^3	25
Pile type	-	-	Predefined massive circular pile
Diameter	D	m	1,5
Area	A	m^2	1,767
Moment of Inertia	I	m^4	0,2485
Out of plane center to center distance of piles	Lspacing	m	3.5
Axial skin resistance	Tskin	kN/m	Layer dependent
Lateral resistance	Tmax	kN/m	938.0
Base Resistance	Fmax	kN	25152.37
Rayleigh	α	-	0.2320
Rayleigh	β	-	8.000E-3

3.3 *Shear Wave Velocity and Soil Type*

The formula for shear wave velocity is given by equation (3):

$$V_S = \sqrt{\frac{G}{\rho}} \tag{3}$$

where V_S = shear wave velocity (in meters per second, m/s); G = shear modulus (also known as the modulus of rigidity, in Pascals, Pa); ρ = density of the material (in kilograms per cubic meter, kg/m³).

To identify soil type from Eurocode 8, the average shear wave velocity of the top 30-meter layer is required. The model provides the shear wave velocity at 30 meters. Therefore, the average shear wave velocity $V_{s,30}$ should be computed using the following expression:

$$V_{s,30} = \frac{30}{\sum\frac{hi}{vi}} = \frac{30}{\left(\frac{30}{170}\right)} = 170.0\ m/s \tag{4}$$

According to Appendix A1, the soil type for this corresponding shear wave velocity is "D". Type D soil represents an envelope of loose-to-medium cohesionless soil having shear wave velocity less than 180 m/s.

4 DYNAMIC ANALYSIS IN PLAXIS 3D

4.1 *Mesh generation*

The minimum average shear wave velocity of the soil profile (Vs, min) is 170 m/s, and the maximum frequency of the input motion is 2 Hz (fmax). The average element size should satisfy the following conditions:

$$Average\ element\ size \leq \frac{V_{s,min}}{8 * f_{max}} \tag{5}$$

Table 6 presents the average element sizes for different mesh distributions, ranging from very coarse to very fine.

Table 6. Average element sizes for different distributions

Element Distribution	relative element size factors (re)	average element size, m
Very coarse	2	70.95
Coarse	1.5	53.22
Medium	1	35.48
Fine	0.7	24.83
Very fine	0.5	17.74

4.2 *Stage Construction*

The table 7 outlines the staged construction for Models 1 and 2, incorporating multiple phases that included structural activation, excavation effects, horizontal load application, and dynamic loading with varying time intervals. This stepwise approach enabled a more accurate representation of the load application process and its impact on foundation performance.

Table 7. Stage construction for Model 1 and 2

Phase	Calculation type	Description
Initial Phase	K0- Procedure	Structures deactivated
Phase I	Plastic	Activated Structure, deactivated excavation to -10 m
Phase II	Plastic	Horizontal load activated; displacement reset to zero
Phase III	Dynamic	Dynamic time interval 5 second
Phase IV	Dynamic	Starts from Phase I, dynamic time interval 10s, displacement reset to zero

5 ANALYSIS AND RESULTS

5.1 *Non-Lineal Soil Behaviour and Site Amplification Analysis*

A non-linear dissipative model was created in PLAXIS 3D using the HS-small model, which incorporates the hysteresis behaviour of soil during an earthquake. Soil parameters were used as provided previously. Two nodes were selected from the generated mesh to observe the results: one at the bed-rock level and another at the surface.

The site amplification factor can be calculated as:

$$A.factor = \frac{Peak\ surface\ acceleration\ (Point\ B)}{Peak\ ground\ acceleration\ (\text{Point A})} = \frac{a,\max(0,t)}{a,\max(H,t)} = \frac{0.027}{0.01} = 2.7 \quad (6)$$

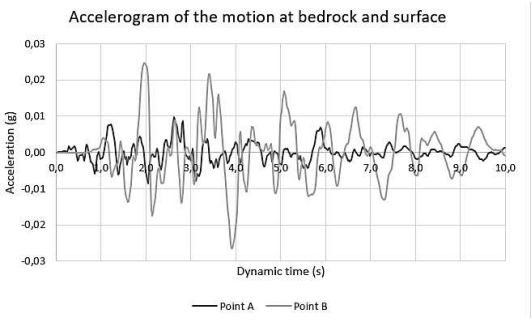

Figure 7. Free field response in terms of acceleration

5.2 *Seismic Response analysis in PLAXIS*

To obtain the response of the structure at base and slab levels, the following nodes were selected.

Table 8. Coordinates of selected nodes

Nodes	Coordinate	Location
A	(38.5, 38.5, -220)	At the bottom of the soil layer
B	(38.5, 38.5, -90)	At the bottom of the pile
C	(38.5, 38.5, -10)	Mid-point of the base
D	(38.5, 38.5, -0.0)	Mid-point of the 1-floor
E	(38.5, 38.5, 255)	Mid-point of the slab for 50-story
F	(38.5, 38.5, 480)	Mid-point of the slab for 100-story

5.3 *Tall building structure with shallow foundation and jet grouting*

The following figures illustrate the result of the dynamic analysis, comparing the response of the shallow foundation with jet grouting under both static and seismic loads.

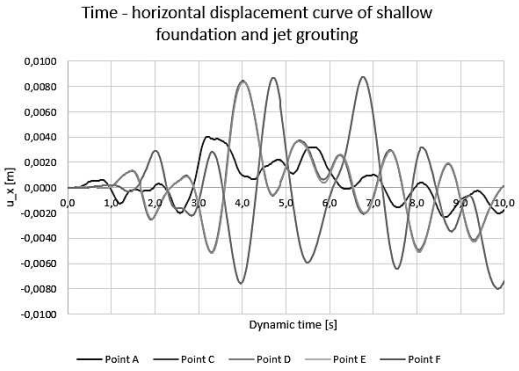

Figure 8. Additional displacements Uz -0,864cm Seismic load

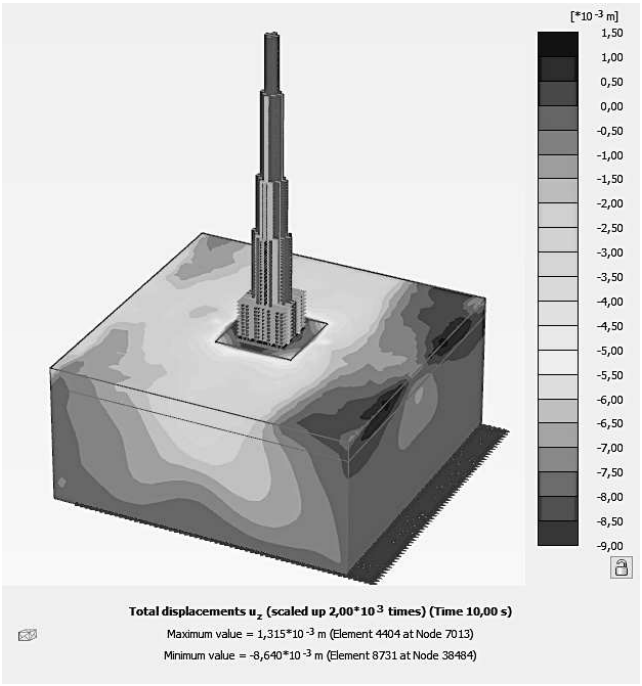

Figure 9. Time-acceleration curve of shallow foundation and jet grouting

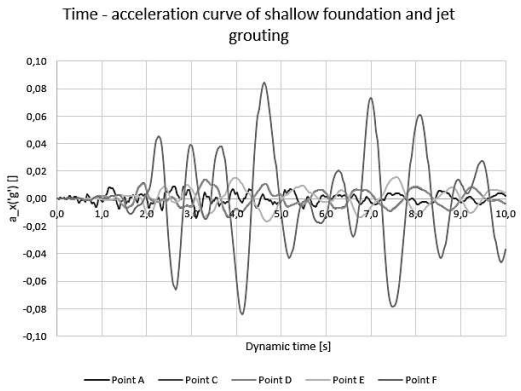

Figure 10. Time-horizontal displacement curve of shallow foundation and jet grouting

5.4 *Tall building structure with piled raft*

The following figures illustrate the result of the piled raft under both static and seismic loads.

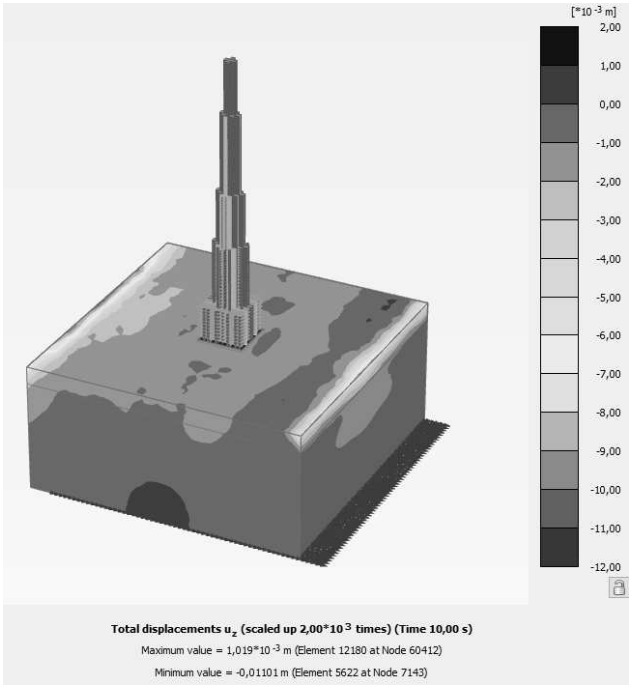

Figure 11. Additional displacements Uz -1,101 cm Seismic load

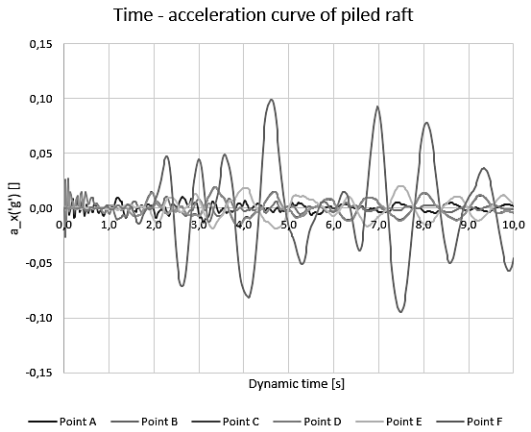

Figure 12. Time-acceleration curve of piled raft

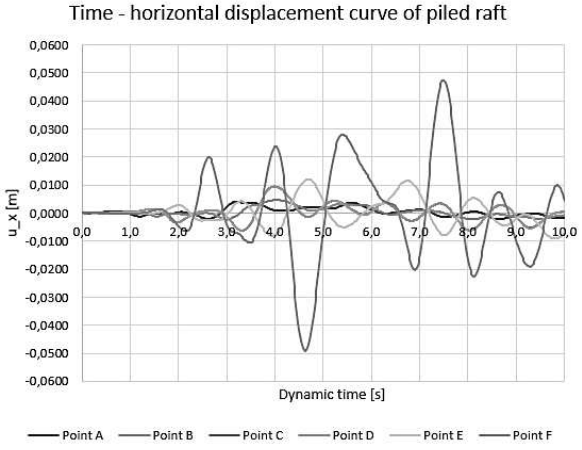

Figure 13. Time-horizontal displacement curve of piled raft

5.5 *Calculation of Shear Force at the shallow base*

The following tables illustrate the result shear force, the acceleration and the horizontal displacements under seismic load.

Table 9. Obtained base shear in the base of the whole structure in kN/m

Eurocode 8	PLAXIS 3D	
q= 1.0	Shallow foundation and jet grouting	Piled raft
11256,7	7765	8206,2

Table 10. Accelerations and horizontal displacements for two types of High-rise building foundations

Coordinates	High-rise building with a shallow foundation and jet grouting		High-rise building with pile-raft	
	a_x('g')	u_x [cm]	a_x('g')	u_x [cm]
Point C	0,018	0,85	0,025	1,25
Point F	0,081	0,90	0,100	5,00

6 CONCLUSIONS

The studied earthquake, with a seismic acceleration of 0.01(g), likely corresponds to a magnitude of less than 3.5, classifying it as a weak earthquake that does not significantly impact buildings or people. However, the increase in seismic acceleration at the ground surface to 0.027(g) is attributed to the effect of a 30-meter layer of weak soil.

This study analysed the seismic response of high-rise buildings with different foundation types in soft soils. The results showed that weak soils amplify seismic acceleration, increasing structural demands. Piled-raft foundations, while improving load-bearing capacity, also transmitted higher accelerations (0.100g vs. 0.081g) and caused greater horizontal displacements (5.00 cm vs. 0.90 cm) compared to shallow foundations with jet grouting.

Base shear calculations indicated that Eurocode 8 may overestimate shear forces for shallow foundations, leading to potentially conservative designs. The presence of piles increased shear forces at the foundation by nearly 10%, highlighting the need for careful seismic design considerations.

Piled-raft foundations enhance structural stability but amplify acceleration transmission, requiring optimized seismic mitigation. In high-seismic zones (0.4g–0.8g), inadequate assessment of soil-structure interaction increases the risk of severe damage or collapse. This is because higher shear forces develop at the base of the high-rise building, while the presence of piles increases seismic acceleration, leading to greater horizontal deformations at the building's upper levels, as demonstrated in this study.

REFERENCES

Hamada, J. 2015. Bending moment of piles on piled raft foundation subjected to ground deformation during earthquake in centrifuge model test. *Paper presented at the 15th Asian Regional Conference on Soil Mechanics and Geotechnical Engineering.*

Hamada, M. 1991. Damage of piles by liquefaction-induced ground displacements. *Paper presented at the Third US Conference Lifeline Earthquake Engineering, Los Angeles, US.*

Hardin, B.O. & Drnevich, V.P. 1972. Shear modulus and damping in soils: Design equations and curves. *ASCE Journal of the Soil Mechanics and Foundations.*

Martin, G.R. & Lam, I.P. 1995. Seismic design of pile foundations: Structural and geotechnical issues. *Paper presented at the Third International Conference on Recent Advancement in Geotechnical Earthquake Engineering and Soil Dynamics, St. Louis, Missouri.*

Mizuno, H. 1987. Pile damage during earthquakes in Japan (1923-1983). *Paper presented at the Geotechnical Engineering Division of the American Society of Civil Engineers in conjunction with the ASCE Convention Atlantic City, New Jersey.*

Teguh, M., Duffield, C.F., Mendis, P.A. & Hutchinson, G.L. 2006. Seismic performance of pile-to-pile cap connections: An investigation of design issues. *Electronic Journal of Structural Engineering* 6.